Available online at www.sciencedirect.com
SCIENCE DIRECT
Diamond & Related Materials 15 (2006) 880–883
DIAMOND AND RELATED MATERIALS
www.elsevier.com/locate/diamond

Photo and field electron emission microscopy, from sulfur doped nanocrystalline diamond films ☆

F.A.M. Koeck [a,*], M. Zumer [b], V. Nemanic [b], R.J. Nemanich [a]

[a] North Carolina State University, Raleigh, NC 27695-8202, USA
[b] Jozef Stefan Institute, SI-1000 Ljubljana, Slovenia

Available online 28 February 2006

Abstract

Room temperature electron emission from carbon and diamond films is usually based on tunnelling effects and can be implemented by application of an electric field to the emitter surface. Field emission from nanocrystalline thin films exhibits intense emission sites but a direct correlation with morphology has not been established. Thus the emission has to be formulated in terms of the electronic structure of the film as well as the geometric structure. Sulfur doped nanocrystalline diamond films were prepared by plasma assisted chemical vapor deposition utilizing 50 ppm hydrogen sulfide in hydrogen (H_2S:H_2) and pure methane (CH_4) as the carbon source. Emission from these films is characterized by individual emitting sites with diameters <100 nm and an emission site density of $\sim 5\times 10^3$ cm^{-2}. This emission character is attributed to field enhancement where a contribution from geometric as well as electronic effects is discussed.

Keywords: Diamond film; Nanocrystalline; Chemical vapor deposition; Field emission; n-type coping; Work function

1. Introduction

Electron emission from nanostructured materials in general has been described in terms of field enhancement effects which results in a strongly localized discharge of electrons from the emitting surface [1]. The most prominent carbon based materials which fall into this category are nanocrystalline diamond films and carbon nanotubes (CNTs). Carbon nanotubes are characterized by a geometrical structure which corresponds to a high aspect ratio, i.e. the length of the typically nm size diameter tube is much larger than the tip radius of curvature [2]. These structures have shown preferred electron emission when exposed to an electric field F_{applied} due to the enhancement of the applied field at the tip of the object. This field enhancement is related to the aspect ratio by $\beta \propto h/r$ where h is the length and r the radius of curvature of the structure. The local electric field at the emitter is then given by $F_{\text{local}} = \beta \cdot F_{\text{applied}}$. The geometric field enhancement factor for a typical nanotube with a diameter of ~10 nm and length of microns can then be estimated to be from 100 to several 1000 s. Reported values for the field enhancement factor fall into this range, however, those values were determined by a fitting procedure using the Fowler–Nordheim equation which describes electron emission due to high applied fields [3]. Evaluating the geometric dimensions of the emitter and comparing it with the results from the Fowler–Nordheim data often revealed a significant discrepancy in the amount of field enhancement predicted from the morphology and that determined from the fitting.

The Fowler–Nordheim equation relates the emission current J to the extraction field F which is applied between the emitter and anode and has the form:

$$J(F) = A'F^2 e^{\frac{-B'\varphi^{3/2}}{F}}, \quad (1)$$

where A' and B' are functions exhibiting a dependence on the electric field F and the work function φ [4]. In the presence of field enhancing structures the applied electric field F is altered at the location of emission by the field enhancement factor β which then replaces F in the Fowler–Nordheim equation by $\beta \cdot F$. Extracting this parameter β is possible by utilizing the

☆ This research was supported by the Office of Naval Research through the TEC MURI.
* Corresponding author. North Carolina State University, Department of Physics, 851 Main Campus Drive, Partners III Rm 151, Raleigh, NC 27695, USA. Tel.: +1 919 515 3417; fax: +1 919 513 0670.
E-mail address: fakoeck@ncsu.edu (F.A.M. Koeck).

0925-9635/$ - see front matter © 2006 Elsevier B.V. All rights reserved.
doi:10.1016/j.diamond.2006.01.008

Fowler–Nordheim plot where the $\ln(J/F)$ is plotted as a function of $1/F$ with the slope of the resulting straight line proportional to β/φ. Therefore, the emitter work function is a crucial input parameter for the computation of β. Determining the value for the work function involves knowledge of material properties at the emission site which can vary from adjacent regions. Additionally, a strongly enhanced localized field can result in significant field penetration which in turn can cause a band bending configuration corresponding to a reduced effective work function. The localized emission from nanostructured carbon films can then be attributed to the local variation in the electronic structure in addition to field enhancement and penetration effects.

In this paper we present results from sulfur-doped nanocrystalline diamond films with respect to electron emission at various fields and temperatures and discuss the origins of the observed individual emission sites.

2. Experimental

Sulfur-doped nanocrystalline diamond films were synthesized by chemical vapor deposition utilizing a mixture of 50 ppm hydrogen sulfide in hydrogen as the dopant source and pure methane as the carbon source. Deposition conditions were 20 Torr chamber pressure and ~900 °C substrate temperature. The film thickness was monitored in situ by laser reflectance interferometry with a final film thickness of ~0.3 μm. The substrate material was polished molybdenum.

The samples were characterized with respect to electron emission employing thermal field emission as well as room temperature emission imaging by an ITO set-up. Both systems are capable of recording the emission current as a function of the applied voltage. A microscopic study was performed utilizing electron emission microscopy in a controlled UHV environment and a lateral resolution better than 10 nm. In addition the instrument, an Elmitec® electron emission microscope, allows temperature dependent imaging of the sample surface positioned 2–5 mm from a perforated anode and with the sample held at −20 kV. An electromagnetic lens column focuses the electrons onto an image intensifier which includes a microchannel plate and a phosphor screen. The resulting image is then captured via a CCD camera [5].

3. Results and discussion

Nanostructured carbon materials, i.e. nanocrystalline diamond, carbon nanotube (CNT) and nano-crystal graphitic films are characterized by nanoscale morphological elements which comprise the deposit. These structures can give rise to properties significantly different than their bulk counterparts of graphite or diamond.

Sulfur-doped nanocrystalline diamond films exhibit a morphology which can be described as diamond or sp^3 bonded carbon grains embedded into a matrix of a graphitic or sp^2 bonded carbon phase. Scanning electron microscopy measurements display a grain dimension of ~100 nm with a superimposed fine structure as shown in Fig. 1. This surface

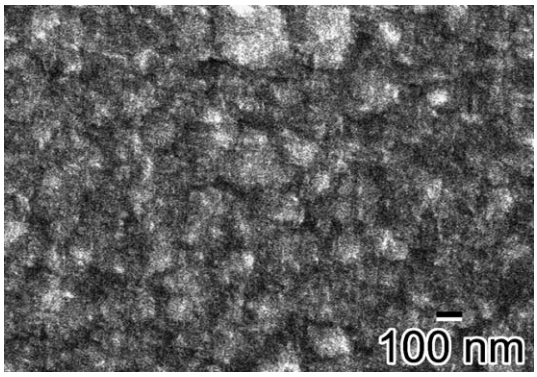

Fig. 1. Scanning electron microscopy image of a sulfur doped nanocrystalline diamond film indicating a grain like film morphology.

structure continues across large deposition areas, here, over a 1 in. diameter disk, where only small variations in surface features across the sample are observed.

The typical roughness of a nanocrystalline diamond film is in the 10 nm range and is of relevance examining field emission characteristics [6]. Structural smoothness and long range structural film uniformity are contrasted by an emission behavior where small, localized sites dominate the electron emission from the surface. While it has been argued that geometric field enhancement is the dominant component in the electron emission characteristics [7], a study correlating morphology and emission sites could not substantiate this proposition [8]. The observed emission behavior and surface morphology, however, indicate that at least a portion of the field enhancement arises from a non-geometric effect. Thus, the geometric field enhancement is determined by the microscopic film morphology where the fine structure of the grains and grain boundaries can result in a field enhancement different from grain size considerations alone. However, small RMS roughness values typical for nanocrystalline diamond films are not expected to give rise to significant field enhancement factors [9].

A large area electron emission projection from a sulfur-doped nanocrystalline diamond film synthesized with 5 sccm H_2S in H_2 and 20 sccm CH_4 is shown in Fig. 2a. In the emission setup, the sample is opposed by a grid structure and an electric field of 2.7 V/μm is established between the vacuum gap of 0.6 mm. Adjacent to the grid an indium-tin-oxide (ITO) screen displays the pattern of the projected electrons. Like other nanostructured carbon films the emission is dominated by emission sites randomly distributed across the surface with a brightness varying over a wide range.

Electron emission microscopy is capable of imaging low intensity sites and an estimate of their size can be specified. The emission sites shown in Fig. 2b have an estimated radius of ~100 nm which is larger than the structural features on the film as determined by scanning electron microscopy (see Fig. 1). Previous results on undoped nanocrystalline diamond films suggested the size of a low intensity emission site to be <10 nm. With an increase in emission site brightness an increase in the projected site image is observed. For electron emission microscopy the focusing condition is dependent on the energy of the emitted electrons. Thus, a non-monochromatic electron beam will exhibit a variation in its focal length resulting in a

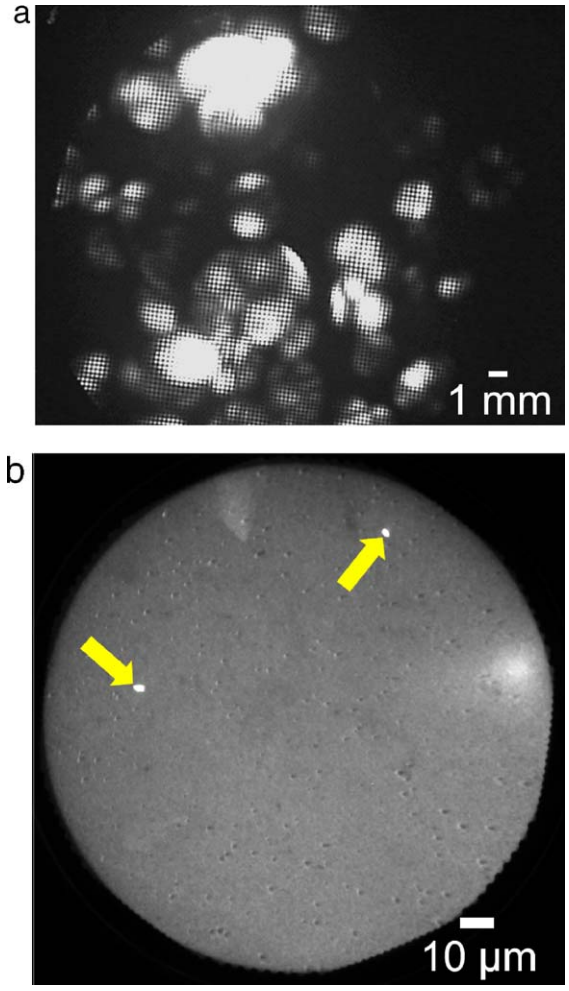

Fig. 2. (a) Large area ITO image of a sulfur-doped nanocrystalline diamond film exhibiting localized emission. (b) Electron emission microscopy image of the same film with 2 emission sites marked by the arrows.

broadened projected site diameter. The FWHM energy width measured from an individual 44 nm diameter multiwall carbon nanotube has been shown to increase linearly with extraction voltage while a 9 nm diameter tube did not exhibit such dependence [10]. This divergence effect may account for the observed emission behavior. The estimated emission site radius of ~100 nm is thus a value for the upper limit of the size of an individual emission site. Results from our direct emission site observation technique is contrasted by results from scanning anode field emission microscopy, where micron sized emission sites have been observed [11].

For a sulfur-doped nanocrystalline diamond film the emission current increases with applied field and temperature. In addition, at elevated temperatures a significant reduction in the threshold field is observed and the emission current increases at a higher rate with the applied field (see Fig. 3A). Recording the emission current as a function of the extraction field and plotting the data with respect to the Fowler–Nordheim relation results in a data-plot shown in Fig. 3B. The Fowler–Nordheim fitting results indicate a significant change of the β/φ ratio with temperature.

One critical result arises from the Fowler–Nordheim approach which suggests a high value for the ratio of the geometric field enhancement factor β and the work function φ. Assuming a work function of ~5 eV (typical for graphite) would result in a geometric field enhancement factor of >5000 in contradiction with the observed sample morphology. Additionally, the geometry of structural features would not exhibit a dependence in the observed temperature range thus ruling out a significant contribution to the temperature dependent emission behavior from a geometric $\beta(T)$.

Photoemission spectroscopy has also been applied to nanocrystalline diamond films and a work function of ~5.8 eV was measured while field emission from the same films displayed a field enhancement factor >1000 [12]. It is evident that photoemission measurements provide the value for the work function typical of all regions on the surface where a variation in the local work function, i.e. at the location of the emission site, is not necessarily captured.

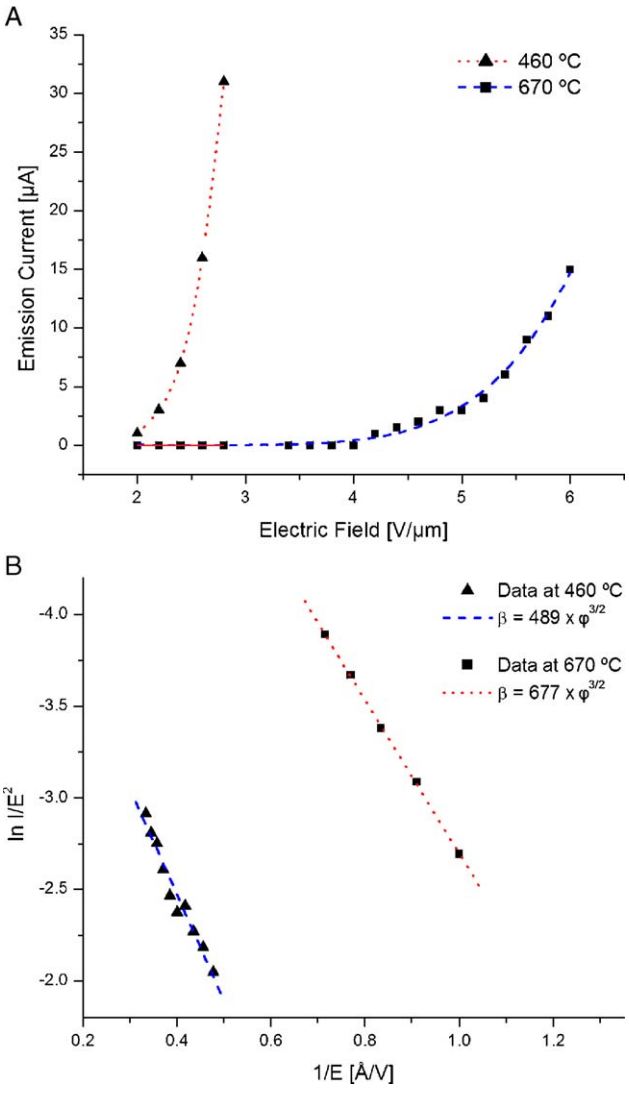

Fig. 3. (A) Electron emission from a sulfur-doped nanocrystalline diamond film at two temperatures. (B) Fowler–Nordheim plot of the emission data with a fit (broken lines) to determine the β/φ ratio.

In a previous study we reported a field enhancement factor <100 for similar sulfur-doped nanocrystalline diamond films [13]. This value was determined by fitting thermionic field emission data to the Schottky emission equation. A different group reported field enhancement factors of β=10–100 for nanocrystalline diamond films [14]. These moderate field enhancement factors can be attributed to the film morphology. However, they cannot provide sufficient barrier lowering to account for the observed emission.

While the Fowler–Nordheim or Schottky equation describe emission under the influence of an electric field they do not consider effects of the applied field penetrating into the emitter. A simulation of the effects of field penetration on a single wall carbon nanotube (SWCNT) has been evaluated [15]. The SWCNT exhibited a geometric field enhancement factor of β=410 at an applied field of 14 V/μm. This was in contrast to the calculated effective field enhancement factor of 1200 where the difference was attributed to field penetration. This high effective field enhancement factor resulted in a significant reduction of the work function from 4.5 eV under zero field to 2.0 eV at 14 V/μm.

We suggest the moderate geometric field enhancement factor of sulfur-doped nanocrystalline diamond films is increased by field penetration effects. With an increase in temperature the emission current is enhanced by thermionic emission and the sites also apparently exhibit a reduced effective work function. The effective field enhancement factor as determined by a Fowler–Nordheim fit incorporates effects due to field penetration.

4. Conclusion

Sulfur-doped nanocrystalline diamond films were synthesized by microwave plasma assisted chemical vapor deposition utilizing a 50 ppm hydrogen sulfide in hydrogen mixture. The samples were characterized with respect to electron emission and exhibited individual emission sites, typically <100 nm site radius, in a random distribution across the sample surface. Scanning electron microscopy images displayed a uniform surface with no distinct protrusions to account for the large field enhancement. Field-thermionic emission measurements with respect to the Fowler–Nordheim relation suggested an effective field enhancement factor significantly larger than its geometric counterpart. We suggest that the discrepancy may be due to field penetration effects which can induce a significant emission barrier lowering and account for the observed emission behavior.

References

[1] V.D. Frolov, A.V. Karabutov, S.M. Pimenov, V.I. Konov, V.P. Ageev, Diamond and Related Materials 10 (9–10) (2001) 1719.
[2] L. Zhua, J. Xub, Y. Xiua, Y. Sunb, D.W. Hessa, C.P. Wongb, Carbon 44 (2) (2006) 253.
[3] C. Zhu, C. Lou, W. Lei, X. Zhang, Applied Surface Science 251 (1–4) (2005) 249.
[4] A. Modinos, Field, Thermionic and Secondary Electron Emission Spectroscopy, Plenum Press, New York, 1984.
[5] H. Ade, W. Yang, S.L. English, J. Hartman, R.F. Davis, R.J. Nemanich, V. N. Litvinenko, I.V. Pinayev, Y. Wu, J.M.J. Madey, Surface Review and Letters 5 (6) (1998) 1257.
[6] H. Yoshikawa, C. Morela, Y. Koga, Diamond and Related Materials 10 (9–10) (2001) 1588.
[7] O. Gröning, L.-O. Nilsson, P. Gröning, L. Schlapbach, Solid-State Electronics 45 (6) (2001) 929.
[8] F.A.M. Köck, J.M. Garguilo, R.J. Nemanich, Diamond and Related Materials 13 (4–8) (2004) 1022.
[9] H. Yoshikawa, C. Morel, Y. Koga, Diamond and Related Materials 10 (9–10) (2001) 1588.
[10] M.J. Fransen, Th.L. van Rooy, P. Kruit, Applied Surface Science 146 (1999) 312.
[11] L. Nilsson, O. Groening, O. Kuettel, P. Groening, L. Schlapbach, Journal of Vacuum Science & Technology B 20 (1) (2002) 326.
[12] O. Groening, O.M. Kuettel, P. Groening, L. Schlapbach, Journal of Vacuum Science & Technology B 17 (5) (1999) 1970.
[13] F.A.M. Koeck, R.J. Nemanich, Diamond and Related Materials 14 (11–12) (2005) 2051.
[14] V.D. Frolov, A.V. Karabutov, S.M. Pimenov, V.I. Konov, Diamond and Related Materials 9 (3–6) (2000) 1196.
[15] X. Zheng, G.H. Chen, Z. Li, S. Deng, N. Xu, Physical Review Letters 92 (2004) 106803.